IMPROVING THE EFFICIENCY OF CONCENTRIC HEAT EXCHANGER USING NANO PARTICLES IN THE FLUID AND TRANSITIONING

Mohamed E. A. Taha[1], Ali I. Shehata[2], Ahmed A. Taha[3] and Mohamed M. Khairat Dawood[4]

(1) *ADES Holding Company, Headquartered in Al Khobar of Saudi Arabia, Mohamed.scct@hotmail.com*

(2) *Mechanical Engineering Department, Arab Academy for Science, Technology and Maritime Transport, Alexandria, Egypt, aliismail@aast.edu*

(3) *Mechanical Engineering Department, Arab Academy for Science, Technology and Maritime Transport, Alexandria, Egypt, aataha82@gmail.com*

(4) *Damanhur University, Mechanical Engineering Department, Faculty of Engineering, Egypt, mohamed_khairat@eng.damnhour.edu.eg*

Keywords: Heat Exchanger, Nano Particles, Heat transfer Cofficient, parallel flow, Counter flow

ABSTRACT: Nanofluids, due to their superior thermal and rheological properties, can be used to increase the shell and tube heat exchanger performance and efficiency. Both parallel and counter flows of acting will be are studied using rotating the inside tube at speed range from 0 to 1500 rpm. The results show a significant improvement in the heat transfer rate due to the swirl effect created by the the turbulence acting as a catalyst. The heat transfer coefficient is enhanced by using the nanoparticles by up to 25% when compared to the base fluid.

2. INTRODUCTION

Heat transfer is a fundamental process in which internal energy is exchanged between two substances, resulting in a transfer of thermal energy. This phenomenon is essential in the analysis of thermodynamic processes, particularly those occurring in heat engines and heat pumps.[1-2]
The shell and tube heat exchanger is one of the most used types of heat exchangers in commercial and industrial applications. It is the most basic, with hot and cold fluids moving in the same direction or in different directions. The shell and tube heat exchanger's capacity to handle products with particles without running the risk of a blockage is a huge advantage.[3-4]

The double pipe heat exchangers are used in the chemical, food, oil and gas industries for pasteurisation, sterilisation, reheating, preheating, digester heating and effluent heating operations, as well as for heating and cooling in sanitary and pharmaceutical applications. Furthermore, because of its inexpensive, easy-to-clean design, and straightforward construction, the double-tube heat exchanger has been widely employed in a variety of renewable energy systems, including air conditioning, geothermal, solar, waste heat recovery, combustion, and latent heat energy storage [5-6].

Improving the heat transfer coefficient of fluids is essential for enhancing heat exchanger performance[7,8].

MARLOG 13

In recent years, nanofluids, which are base fluids containing solid particles with high thermal conductivity at the nanoscale, [9-11]. have been employed to enhance the thermo-physical properties of fluids. Various types of nanoparticles, including silicon carbide, graphene, and aluminum oxide, have been studied for their impact on heat exchanger performance. [12].Researchers have explored the addition of nanofluids in different heat exchanger types, such as double pipe, shell-tube, and plate heat exchangers.

Studies have shown that nanofluids can significantly improve the heat transfer coefficient, with experiments involving different process parameters and nanofluid type variations[13-18].

Khan et al. [19] experimentally analyzed a photovoltaic-thermal system using Fe3O4/SiO2 hybrid nanofluids. The nanofluids provided superior cooling and efficiency compared to base fluids, with optimal performance at 3% concentration and 40 LPM flow rate.

For example, experiments with Al_2O^3 nanoparticles in a double pipe heat exchanger increased the thermal conductivity of the fluid. [20].Other studies investigated the influence of nanofluids on heat transfer in microchannel heat exchangers, indicating notable improvements in heat transfer coefficients [21].

Research has also delved into modifying geometrical shapes of heat exchangers such as adding longitudinal fins, helical coils, and spiral-shaped double tubes resulting in positive impacts on performance[16]. Numerical investigations on conical tube double pipe heat exchangers and optimal design parameters using techniques like Response Surface Method (RSM) have been explored[27,28]. Additionally, studies on shell-and-tube heat exchangers considered factors like baffle cut and spacing have been studied and showed better performance compared by

Henein et al. used a MgO/MWCNT-water hybrid nanofluid as a working fluid to improve the thermal performance of a heat-pipe evacuated-tube solar collector with a concentration of 0.02% at volume flow rates ranging from 1 to 3 L/min. The energy and energy efficiencies were found to improve when the volume flow rate and weight ratios of the MWCNT nanoparticles increased. The MgO/MWCNT (50:50) hybrid nanofluid improved the collector's energy and energy efficiency by 55.83% and 77.14%, respectively [22-29].

Specifically, papers focusing on double pipe heat exchangers with nanofluids highlighted improvements in convective heat transfer coefficients [30].Results from experiments with alumina nanoparticles and transformer oil showed increased heat transfer coefficients with higher solid concentrations [31].Other studies examined the impact of water/CuO nanofluid on convection heat transfer coefficients, demonstrating improvements with increased Reynolds number and nanoparticle volume fraction[32].

As previously stated, practically all research efforts have been focused entirely on enhancing the heat transfer coefficient. They haven't, however, stressed how crucial it is to reduce or stay away from pressure decreases. Furthermore, to the best of our knowledge, research on the application of nanofluids in heat exchangers only supports variables that impact heat transfer, with little to no discussion if any of the variables that effect pressure drop being carefully examined. Thus, this review's primary goal is to examine the variables that affect nanofluid performance in heat exchangers in order to enhance heat transfer and reduce or prevent significant increase in the pressure drop.

3. HEAT EXHCANGER SYSTEM DESIGN

Enhancing the heat transfer rate and preventing or minimising a significant pressure loss are the two main functions of a double-pipe heat exchanger. Since it suggests a smaller pressure drop, a fluid with a high viscosity value is often best suited for the side with the bigger passage area (annular) [11]. A double-pipe heat exchanger diagram is shown in Figure 1. The simplest heat exchanger concept is one in which hot and cold fluids circulate in the same or opposite directions through a double-pipe design. While the other fluid travels via the annular gap between two tubes, the first fluid passes through the smallest tube.

There are two alternative configurations for the flow: the first uses both fluids in parallel flow, where the hot and cold fluids enter at the same borders and flow in the same direction (Figure 1a). In the alternative configuration (Figure 1b), fluids arrive in counterflow, travelling in opposite directions, at opposite inlets [12-20]. The advantages of using the concentric tube heat exchangers are their simple design, ease of cleaning, suitability for handling dirty fluids, ability to operate under high pressure, [21].and the promotion of turbulent flow at low rates, leading to enhanced heat transfer efficiency.
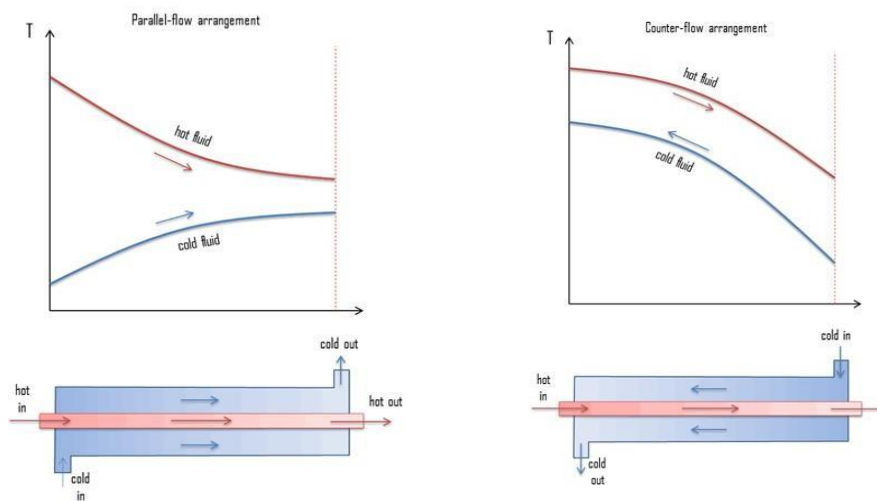

Figure (1)Double-pipe heat exchangers using (a) parallel flow and (b) counter flow.

Concentric tube heat exchangers have two main configurations: parallel flow and counter flow. [31] In the parallel flow arrangement [28], both hot and cold fluids enter the heat exchanger from the same end, flow in the same direction, and exit from the same end. On the other hand, in the counter flow arrangement, the fluids enter from opposite ends, [33] flow in opposite directions, and exit from opposite ends. At the same conditions more heat is transferred in the counter flow than parallel flow [29]. The main disadvantages of using parallel flow in heat exchangers are the occurrence of large thermal stresses due to significant temperature differences between the inlet and outlet[34-35].

In contrast, counter flow is preferred because it minimizes thermal stresses, [28] ensures more uniform heat transfer, [36-38] also the outlet temperature of the cold fluid approaches highest temperature of the hot fluid as in Figure 1-b And allows the outlet temperature of the cold fluid to approach the highest temperature of the hot fluid. [39]Counter flow arrangements generally require a smaller heat exchanger surface area for the same rate of heat transfer compared to parallel flow.

4. PREPARATION OF TIO2/WATER NANOFLUID

The average diameter of the TiO2 nanoparticles, which measured 12 nm, was obtained from Nanostructured and Amorphous Material, Inc. in the United States. TiO2 nanoparticles were distributed at three distinct concentrations of ϕ = 2%, 3%, and 5% by volume in de-ionized water, the base fluid, prior to testing. Subsequently, the mixture was subjected to continuous sonication for 180 minutes at 36 ± 3 kHz using ultrasonic pulses of 100 W to achieve homogeneous particle dispersion. Furthermore, the stability of suspension was markedly enhanced by the sonication treatment. As a result, before being fed into the tube.

5. EXPERIMENTAL TEST RIG

Figures. 2 & 3 depict the current study's experimental setup. A heat exchanger tube, two cooling water tanks, an overhead fluid tank, three thermocouples, a data recorder, a manometer, a centrifugal pump, seven rotameters, eight multimeters, and nine variac transformers made comprised the facility's principal components. The copper tube measured 19 mm in diameter (D), 1000 mm in length (L), and 1.5 mm in thickness (t). A tranquil section's length was determined to be 1200 mm. An electrical heater wire wrapped around a circular tube provided a constant wall heat flux boundary condition for the heat transfer experiment. A variac transformer was used to regulate the electrical output power.

The tested tube's exterior was well-insulated to reduce convective heat loss to the surrounding area. Prior to testing, the inlet and exit temperatures of the bulk fluid were monitored and recoded at specific times using a data logger and RTDs calibrated within ±0.2°C deviation by thermostat. Type T thermocouples were used to measure fifteen local temperatures on the test tube's upper, bottom, and side walls.

Figure (2) 3D representation of Heat Exchanger including the measuring equipments

During the trials, a 1.0 hp centrifugal pump moved incoming bulk fluids at 26 °C via a fluid setting tank, rotameter, and heat transfer test tube. An electrical heater that could be adjusted was wrapped around the test tube to heat the bulk fluids. The bulk fluids' temperature, volumetric flow rate, and pressure drop were measured under steady state conditions. The fluid's inlet Reynolds number was adjusted between 1000 and 25,200. The average tube wall temperature and the fluid temperatures at the inlet and outflow served as the basis for the fluid characteristics used in the flow and heat transfer studies. Note that the heat transfer test tube's pressure drop was measured using a manometer in an isothermal environment, without switching on the heating unit. In the experiments, different volume concentrations of TiO2 nanoparticles of ϕ = 1%, 3% and 5% by volume were examined for both parallel and counter flow (Table 1).
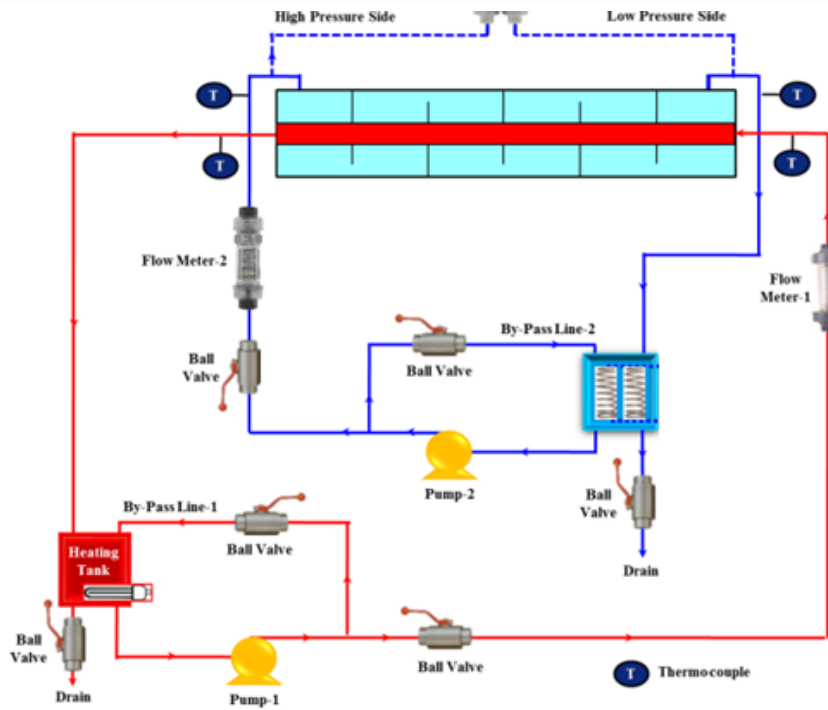
Fig. 3. Layout of the experimental setup.

The process of assembling the heat exchanger was mainly the work of connecting the hose to the pumps and the tanks. So, the device can be used for both parallel and counter flow. The other arrangement depends on directing the inlet flow whether it introduced to the heat exchanger in direction tangential to the hot pipe or perpendicular to the hot pipe.

6. DATA REDUCTION

6.1. THERMOPHYSICAL PROPERTIES OF NANOFLUIDS

The thermophysical properties (density, specific heat, viscosity and thermal conductivity) of the nanofluid were calculated as a function of nanoparticle volume concentration (ϕ) together with properties of base fluid and nanoparticles. The density of nanofluid was evaluated using the general formula for the mixture:

$$\rho_{nf} = (1 - \phi)\rho_{water} + \phi\rho_{np} \tag{4}$$

The specific heat of the nanofluid was evaluated from.

$$C_{p,nf} = \frac{\phi\,\rho_{np}C_{p,np} + (1 - \phi)\rho_{water}\,C_{p,water}}{\rho_{nf}} \tag{5}$$

These equations were recommended for nanofluids through experimental validation by Pak and Cho [2] and Xuan and Roetzel [40-42]. The thermal conductivity was calculated from Maxwell model [43] as shown in Eq. (6) which was recommended for homogeneous and low volume concentration liquid–solid suspensions with randomly dispersed, uniformly sized and non-interacting average spherical particles [44-46].

$$\frac{k_{nf}}{k_{water}} = \frac{k_{np} + 2k_{water} + 2\phi\left(k_{np} - k_{water}\right)}{k_{np} + 2k_{water} - \phi\left(k_{np} - k_{water}\right)} \qquad (6)$$

Viscosity of nanofluids was calculated via the general Einstein's formula [45].

$$\mu_{nf} = \mu_{water} + \left(1 + \eta\,\phi\right) \qquad (7)$$

Where $\eta = 2.5$, as recommended for hard spheres [44].

6.2. CALCULATION OF THE HEAT TRANSFER

In the present work, the heat transfer rate of working fluids was calculated by using the difference between inlet and outlet working fluid temperatures as

$$Q_{fluid} = M_{Cp}\left(T_o + T_i\right) \qquad (8)$$

The thermal equilibrium test showed that the heat supplied by electrical winding in the test section is 5–8% larger than the heat absorbed by the working fluid.

$$\left|\frac{Q_{IV} - Q_{fluid}}{Q_{IV}}\right| \times 100\% \leq 5 - 8\% \qquad (9)$$

At the steady-state rate, the heat transfer taken by the fluid is equal to the convection heat transfer from the test section which can be expressed as

$$Q_{fluid} = Q_{conv} \qquad (10)$$

Where

$$Q_{conv}\, h\, A\left(\tilde{T}_w - T_b\right) \qquad (11)$$

where Q_{conv} is the convection heat transfer from the test section, A is the heating internal surface area, T_b is average fluid bulk temperature in the tube and T_w is average wall temperature lined between the inlet and the exit of the test tube.

$$\tilde{T}_w = \sum T_w / 15 \qquad (12)$$

where T_w is the local wall temperature and evaluated at the outer wall surface of the test tube. The average heat transfer coefficient (h) was determined by combining Eqs. (8) and (11) as

$$h = M_{Cp}\left(T_o + T_i\right) / A\left(\tilde{T}_w - T_b\right) \qquad (13)$$

For the local heat transfer coefficient, the bulk-fluid and wall temperatures were selected from a specific local station. Nusselt number is calculated using the following equation;

$$Nu = h\,D / k \qquad (14)$$

where D is the inner test tube and k is the thermal conductivity of the fluid (water/nanofluid).

6.3. CALCULATION OF THE FRICTION FACTOR

The pressure drop (ΔP) across the test section length (L) is calculated from the difference of the levels of manometer fluid. Then pressure drop data were subjected to the calculation of friction factor via the following equation;

$$f = \left(D/L\right)\left(2\,\Delta P / \rho U^2\right) \qquad (15)$$

where U is average velocity that calculated by dividing the measured volumetric water/nanofluid flow rate by the inlet cross-section area (A).

The Reynolds number based on inner test tube diameter is given by

$$Re = \rho U\,D / \mu \qquad (16)$$

All of the thermo-physical properties (k, ρ, μ, c_p) used for the calculation of the dimensionless number (Nu and Pr) are all evaluated at the bulk fluid temperature (T_b) from Eq. (17).

$$T_b = \left(T_o + T_i\right) / 2 \qquad (17)$$

7. Results and Discussion

In this section, the effects of TiO2/water nanofluids on the heat transfer and thermal performance factor characteristics are reported. The results of water (the base fluid) in the plain tube are also reported for comparison for bpoth parallel and counter flows.

Firstly, the heat transfer results of the present tube will be presented for parallel flow by comparing the Nusselt numbers with those obtained from using of Dittus–Boelter and present friction factors with those obtained from Petukhov correlation [47] and Blasius TiO2/water nanofluids correlation [47].
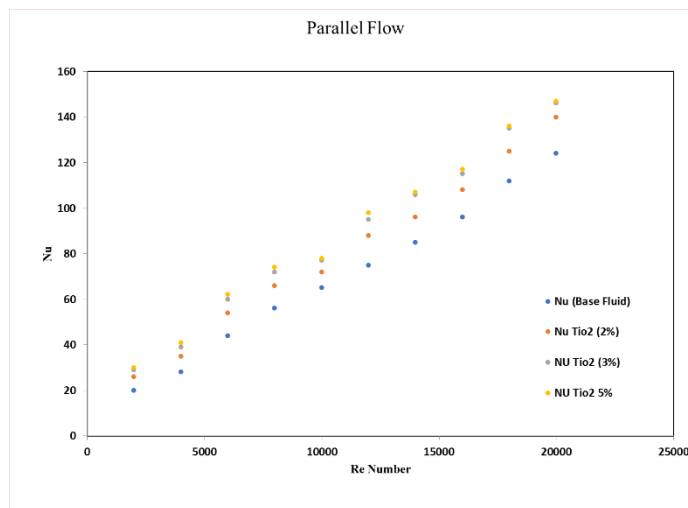

Fig. 4. Effect of nanofluid concentration on heat transfer rate [Nu] for parallel flow

The heat transfer result in Fig. 4 indicates that Nusselt number (Nu) consistently increased with increasing Reynolds number for the parallel flow. At a given Reynolds number, the addition of Tio2 nano particles had higher than the base fluid. The superior heat transfer of this case can be attributed to the 5% Tio2 nanofluid for most of RE range which means that increasing the swirl flow inside the tube. It was also found that heat transfer increased as the tio2 nanofluid concentration increased. As indicated by Nusselt number ratio (Nu base nanofluid /Nu base fluid), for 2%, 3 % and 5 %, respectively resulted in heat transfer enhancement of 30 % , 45 % and 50 % of the plain tube. To assess the effect of twisted tape modification,Obviously, all tested concentration of the nanofluid gave better heat transfer than base fluid. This can be explained by the fact that the dual swirl flows generated by the addition of the nanofluid give better fluid mixing and more efficient thermal energy

performance than the base fluid for parallel flow. The maximum nusslet number is 147 at RE 2000 for the 5 % tio2 nanfluid.
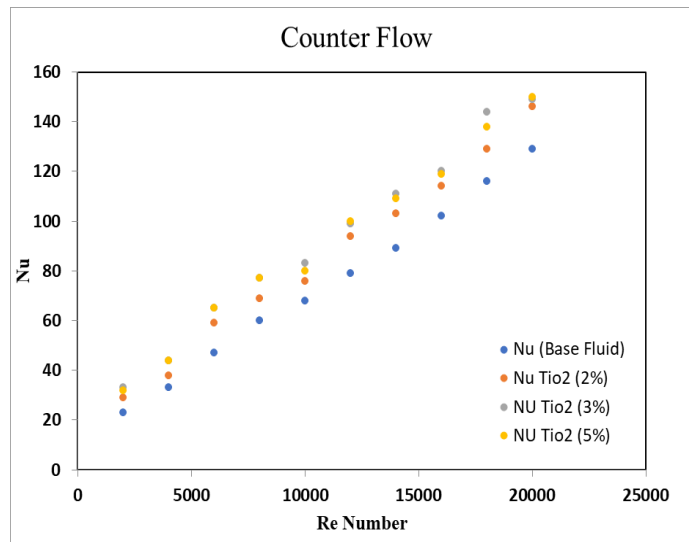

Fig. 5. Effect of nanofluid concentration on heat transfer rate [Nu] for counter flow

The heat transfer result in Fig. 5 indicates that Nusselt number (Nu) again consistently increased with increasing Reynolds number for the counter flow. At a given Reynolds number, the addition of Tio2 nano particles had higher than the base fluid. The superior heat transfer of this case can be attributed to the 5% Tio2 nanofluid till RE reaches 15000 which means that increasing the swirl flow inside the tube. After Re equals 15000, the heat transfer for 3% Tio2 nanofluid is more than that of 5 % Tio2. It was also found that heat transfer increased as the tio2 nanofluid concentration increased. As indicated by Nusselt number ratio (Nu base nanofluid /Nu base fluid), for 2%, 3 % and 5 %, respectively resulted in heat transfer enhancement of 32 % , 48 % and 52 % of the plain tube. All tested concentration of the nanofluid gave better heat transfer than base fluid. This can be explained by the fact that the dual swirl flows generated by the addition of the nanofluid give better fluid mixing and more efficient thermal energy performance than the base fluid for counter flow. The maximum nusslet number is 150 at RE 2000 for the 5 % tio2 nanfluid.
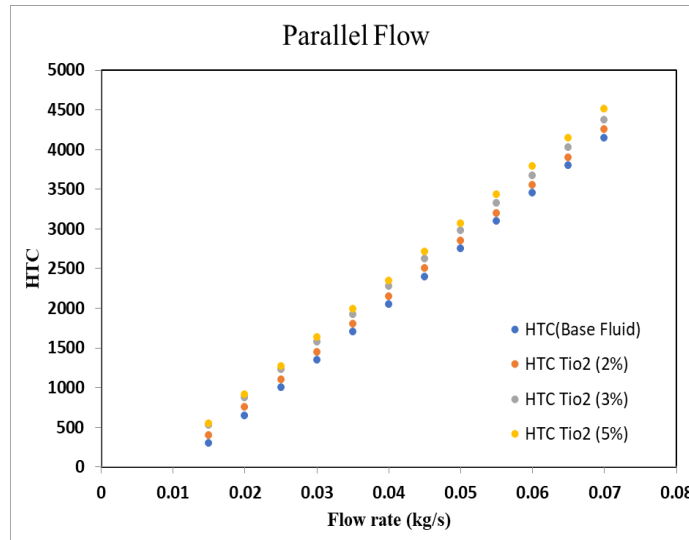
Fig. 6. Effect of nanofluid concentration on heat transfer Cofficient [HTC] for parallel flow

The increase in temperature promoted an increase in the effectiveness (ε) of the heat exchanger and the heat trnfer coefficient as can be seen in Fig. 6. This behavior is related to the alteration of the thermophysicalproperties of the used nano fluid, influenced by the temperature variation. The incrase of the flow rate showed an increment of 60% in HTC using 5% Tio2 nanofluid with the increase in flow rate from 0.02 to 0.07 kg /s, while for the water base fluid, this increment was 35%. The figure shows the variation of HTC concerning the volumetric flow of the fluids. It is also noticed, as expected, the increment of HTC with the increase of the flow for the use of Tio2 nanofluid compare by the base fluid for the parallel flow. As indicated by heat transfer cofficient ratio (HTC nanofluid /HTC base fluid), for 2%, 3 % and 5 %, respectively resulted in heat transfer enhancement of 37 % , 53 % and 62 % of the plain tube for the parallel flow.
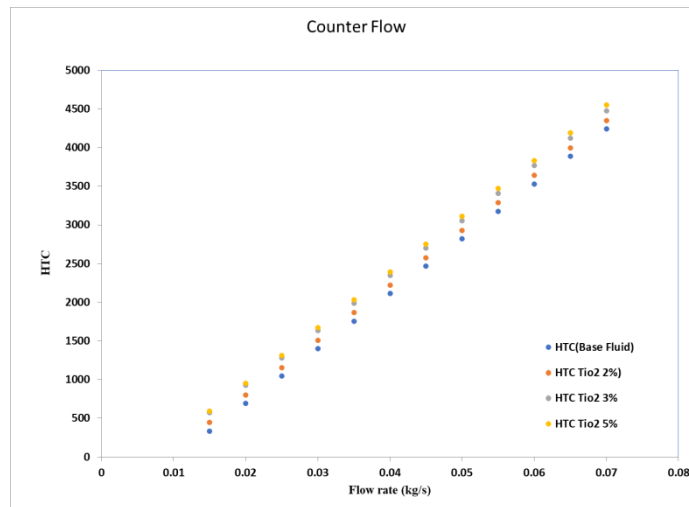
Fig. 7. Effect of nanofluid concentration on heat transfer Cofficient [HTC] for counter flow

In the case of of using nanofuids, in the case of water (as well as the other properties of water), Figure 7 shows an increase in the thermal conductivity concerning the increase in temperature, which is consistent with the literature.[44] Increases in thermal conductivity increase the values of the convection heat transfer coefcient (h), and, consequently, the heat transfer cofficient (HTC) and the efectiveness of the heat exchanger (ε). Regarding the addition of nanoparticles to double-distilled water, a higher concentration of nanoparticles (Tio2 Nanofuid) provide an increase in thermal conductivity concerning the base fuid with higher temperatures, due to degradation of the surfactant with increasing temperature [29]. It is noticed also that the increase in the inlet temperature of the hot fuid intensifed the thermal difusivity and caused a decrease in the viscosity of the fuids; in this way, an increase in the efectiveness of the heat exchanger as shown in the increase of the heat transfer coefficient.The incrase of the flow rate showed an increment of 65% in HTC using 5% Tio2 nanofluid with the increase in flow rate from 0.02 to 0.07 kg /s, while for the water base fluid, this increment was 40%. The figure shows the variation of HTC concerning the volumetric flow of the fluids. It is also noticed, as expected, the increment of HTC with the increase of the flow for the use of Tio2 nanofluid compared by the base fluid for the counter flow. As indicated by heat transfer cofficient ratio (HTC nanofluid /HTC base fluid), for 2%, 3 % and 5 %, respectively resulted in heat transfer enhancement of 42 % , 58 % and 68 % of the plain tube for the counter flow.
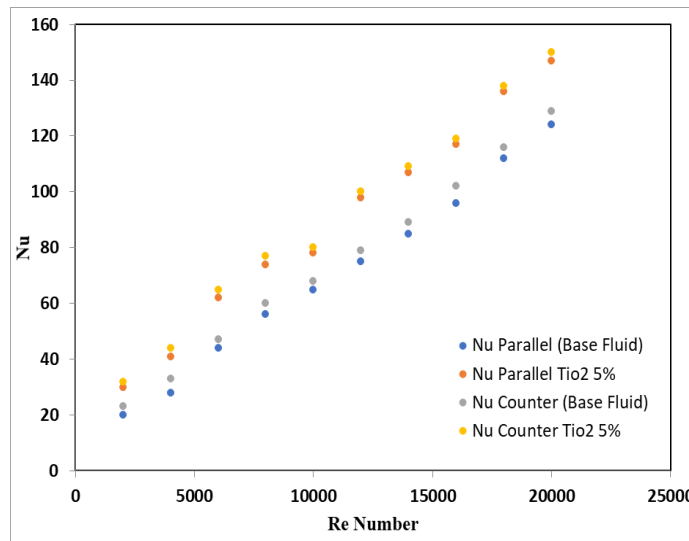
Fig. 8. Effect of flow behavoir on heat transfer rate [Nu] for
Base fluid and Tio2 (5%)

Fig.8 shows the effect of flow behavoir with the addation of 5 % TiO2/water nanofluid on Nusselt number of the tube. For the studied range, Nusselt number increased with increasing TiO2 concentration and all TiO2/water nanofluids gave higher Nusselt number than water as the based fluid. The higher heat transfer by nanofluids arises from: (i) the ability of suspended nanoparticles enhancing thermal conductivity; (ii) movement of nanoparticles delivering energy exchange. The higher volume concentration of nanoparticles would increase thermal conductivity nd contact surface, thus increasing heat transfer rate. The figure also shows that the counter flow give higher Nusselt number than the parallel flow for both the based fluid and using 5 % TiO2/water nanofluid.This can be explained by the fact that the swirl flows generated by the counter flow give better fluid mixing and more efficient thermal disruption than the parallel flow.
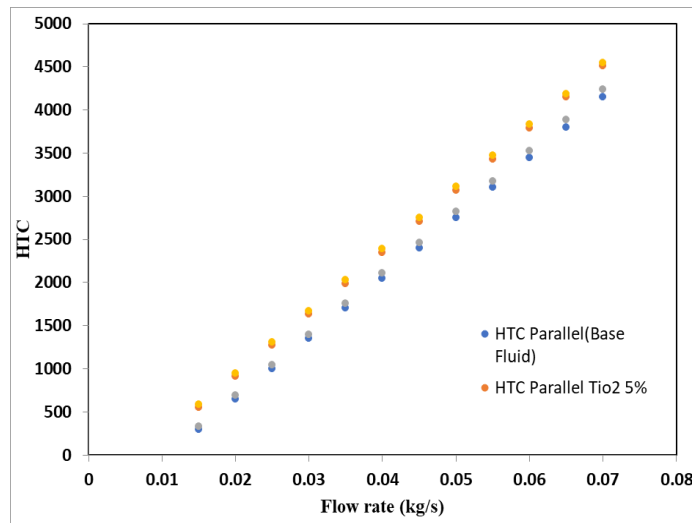
Fig.9. Effect of flow behavoir on heat transfer Cofficient [HTC] for
Base fluid and Tio2 (5%)

Fig. 9 depicts the effect of flow behavoir with the addation of 5 % TiO2/water nanofluid on heat transfer Cofficient [HTC] of the tube. At higher number of flow rate of 0.07 kg/sec, the maximum heat transfer Cofficient [HTC] increased from 4150 to 4240 for the based fluid (water) when changed from paraalel flow to counter flow and 4510 to 4550 from parllel flow to counter flow when the based fluid (water) was replaced by the nanofluids with for TiO2 concentrations of 5%.

8. CONCLUSION

The experimental investigation involving TiO2/water nanofluid for both paraalel and counter flow has unveiled key insights regarding their impact on heat exchanger (HE) performance.

- The obtained results indicated that the counter flow played an important role in improving fluid mixing and heat transfer enhancement.

- Nusselt number, friction factor and thermal performance increased with increasing the flow rate and increasing TiO2 volume concentration.

- The heat transfer cofficient ratio (HTC nanofluid /HTC base fluid) by using TiO2/water nanofluid 2%, 3 % and 5 %, respectively resulted in heat transfer enhancement of 37 % , 53 % and 62 % for the parallel flow compared by 42 % , 58 % and 68 % for the counter flow.

- The maximum thermal performance Nusslet number of 150 was obtained by the use of 5 % TiO2/water Nanofluid for counter flow the maximum heat transfer coefficient (HTC) of 4550

MARLOG 13

was reached by the use of 5 % TiO2/water Nanofluid for counter flow compared with the parallel flow.

9. REFERENCES

[1] S.M. Ammar, et al., Condensing heat transfer coefficients of R134a in smooth and grooved multiport flat tubes of automotive heat exchanger: an experimental investigation, Int. J. Heat Mass Tran. 134 (2019) 366–376, https://doi.org/10.1016/j.ijheatmasstransfer.2019.01.047.

[2] X. Han, N. Chen, J. Yan, J. Liu, M. Liu, S. Karellas, Thermodynamic analysis and life cycle assessment of supercritical pulverized coal-fired power plant integrated with No.0 feedwater pre-heater under partial loads, J. Clean. Prod. 233 (2019) 1106–1122, https://doi.org/10.1016/j.jclepro.2019.06.159.

[3] M.M. Sarafraz, M.R. Safaei, M. Goodarzi, B. Yang, M. Arjomandi, Heat transfer analysis of Ga-In-Sn in a compact heat exchanger equipped with straight micropassages, Int. J. Heat Mass Tran. 139 (2019) 675–684, https://doi.org/10.1016/j.ijheatmasstransfer.2019.05.057 .

[4] E.I. Jassim, Exergy analysis of petrol engine accommodated nanoparticle in the lubricant system, Int. J. Exergy 35 (2021) 406–420.

[5] Esam I. Jassim, Faizan Ahmed, Bashar Jasem, Effect of Mixing Nano-Additive with Engine Oil on the Heat Transfer Performance, International Petroleum Technology Conference, 2020.

[6] A. Bhattad, J. Sarkar, P. Ghosh, Improving the performance of refrigeration systems by using nanofluids: a comprehensive review, Renew. Sustain. Energy Rev. 82 (2018) 3656–3669.

[7]] E.Y. Gürbüz, A. Sozen, ¨H.˙ I. Variyenli, A. Khanlari, A.D. Tuncer, A comparative study on utilizing hybrid-type nanofluid in plate heat exchangers with different number of plates, J. Braz. Soc. Mech. Sci. Eng. 42 (2020) 524, https://doi.org/10.1007/s40430-020-02601-1.

[8]] B. Ali, R.A. Naqvi, L. Ali, S. Abdal, S. Hussain, A comparative description on time-dependent rotating magnetic transport of a water base liquid H2O with hybrid nano-materials Al2O3-Cu and Al2O3-TiO2 over an extending sheet using Buongiorno model: finite element approach, Chin. J. Phys. 70 (2021) 125–139, https://doi.org/10.1016/j.cjph.2020.12.022.

[9] L. Ali, X. Liu, B. Ali, S. Mujeed, S. Abdal, S.A. Khan, Analysis of magnetic properties of nano-particles due to a magnetic dipole in micropolar fluid flow over a stretching sheet, Coatings 10 (2020), https://doi.org/10.3390/coatings10020170.

[10] L. Ali, X. Liu, B. Ali, S. Mujeed, S. Abdal, A. Mutahir, The impact of nanoparticles due to applied magnetic dipole in micropolar fluid flow using the finite element method, Symmetry 12 (2020), https://doi.org/10.3390/sym12040520.

[11] L. Ali, X. Liu, B. Ali, Finite element analysis of variable viscosity impact on MHD flow and heat transfer of nanofluid using the cattaneo–christov model, Coatings (2020) 10, https://doi.org/10.3390/coatings10040395.

[12] H. Eshgarf, R. Kalbasi, A. Maleki, M.S. Shadloo, A. karimipour, A review on the properties, preparation, models and stability of hybrid nanofluids to optimize energy consumption, J. Therm. Anal. Calorim. (2020), https://doi.org/10.1007/s10973-020-09998- w. Jul.

[13] M. Ghalandari, M. Irandoost Shahrestani, A. Maleki, M. Safdari Shadloo, M. El Haj Assad, Applications of intelligent methods in various types of heat exchangers: a review, J. Therm. Anal. Calorim. (2021), https://doi.org/10.1007/s10973-020-10425-3. Jan.

[14] H. Masuda, A. Ebata, K. Teramae, Alteration of thermal conductivity and viscosity of liquid by dispersing ultra-fine particles (dispersion of Al2O3, SiO2 and TiO2 ultra-fine particles), Netsu Bussei 4 (1993) 227–233.

[15] Y. Xuan, Q. Li, Heat transfer enhancement of nanofluids, Int. J. Heat Fluid Flow 21 (2000) 58–64.

[16] D. Zheng, J. Wang, Z. Chen, J. Baleta, B. Sund´en, Performance analysis of a plate heat exchanger using various nanofluids, Int. J. Heat Mass Tran. 158 (2020) 119993, https://doi.org/10.1016/j.ijheatmasstransfer.2020.119993.

[17] A. Sozen, ¨ A. Khanları, E. Çiftçi, Heat transfer enhancement of plate heat exchanger utilizing kaolin-including working fluid, Proc. Inst. Mech. Eng. Part J. Power Energy. 233 (2019) 626–634, https://doi.org/10.1177/0957650919832445.

[18] M.M. Sarafraz, M.R. Safaei, Z. Tian, M. Goodarzi, E.P. Bandarra Filho, M. Arjomandi, Thermal assessment of nano-particulate graphene-water/ethylene glycol (WEG 60:40) nano-suspension in a compact heat exchanger, Energies (2019) 12, https://doi.org/10.3390/en12101929.

[19] Khan AA, Danish M, Rubaiee S, Yahya SM. Insight into the inves- tigation of Fe3O4/SiO2 nanoparticles suspended aqueous nano- fluids in hybrid photovoltaic/thermal system. Clean Eng Technol. 2022. https://doi.org/10.1016/J.CLET.2022.100572.

[19] M. Goodarzi, et al., Investigation of heat transfer performance and friction factor of a counter-flow double-pipe heat exchanger using nitrogen-doped, graphenebased nanofluids, Int. Commun. Heat Mass Tran. 76 (2016) 16–23, https://doi.org/10.1016/j.icheatmasstransfer.2016.05.018.

[20] A. Khanlari, A. Sozen, ¨ H.˙ I. Variyenli, Simulation and experimental analysis of heat transfer characteristics in the plate type heat exchangers using TiO2/water nanofluid, Int. J. Numer. Methods Heat Fluid Flow 29 (2019) 1343–1362, https://doi.org/10.1108/HFF-05-2018-0191.

[21] M. Goodarzi, et al., Investigation of heat transfer and pressure drop of a counter flow corrugated plate heat exchanger using MWCNT based nanofluids, Int. Commun. Heat Mass Tran. 66 (2015) 172–179, https://doi.org/10.1016/j.icheatmasstransfer.2015.05.002.

[22] M.H. Bahmani, O.A. Akbari, M. Zarringhalam, G. Ahmadi Sheikh Shabani, M. Goodarzi, Forced convection in a double tube heat exchanger using nanofluids with constant and variable thermophysical properties, Int. J. Numer. Methods Heat Fluid Flow 30 (2019) 3247–3265, https://doi.org/10.1108/HFF-01-2019- 0017.

[23] M.H. Bahmani, et al., Investigation of turbulent heat transfer and nanofluid flow in a double pipe heat exchanger, Adv. Powder Technol. 29 (2018) 273–282, https://doi.org/10.1016/j.apt.2017.11.013.

[24] Z.X. Li, U. Khaled, A.A.A.A. Al-Rashed, M. Goodarzi, M.M. Sarafraz, R. Meer, Heat transfer evaluation of a micro heat exchanger cooling with spherical carbonacetone nanofluid, Int. J. Heat Mass Tran. 149 (2020) 119124, https://doi.org/10.1016/j.ijheatmasstransfer.2019, 119124.

[25] S.K. Das, N. Putra, P. Thiesen, W. Roetzel, Temperature dependence of thermal conductivity enhancement for nanofluids, J. Heat Tran. 125 (2003) 567–574.

[26] R. Hosseinnezhad, O.A. Akbari, H.H. Afrouzi, M. Biglarian, A. Koveiti, D. Toghraie, Numerical study of turbulent nanofluid heat transfer in a tubular heat exchanger with twin twisted-tape inserts, J. Therm. Anal. Calorim. 132 (2018) 741–759.

[27] N. Putra, W.N. Septiadi, G. Julian, A. Maulana, R. Irwansyah, An experimental study on thermal performance of nano fluids in microchannel heat exchanger, Int. J. Technol. 2 (2013) 167–177.

[28] A.K. Tiwari, P. Ghosh, J. Sarkar, Particle concentration levels of various nanofluids in plate heat exchanger for best performance, Int. J. Heat Mass Tran. 89 (2015) 1110–1118, https://doi.org/10.1016/j.ijheatmasstransfer.2015.05.118.

[29] Henein, S.M.; Abdel-Rehim, A.A. The performance response of a heat pipe evacuated tube solar collector using MgO/MWCNT hybrid nanofluid as a working fluid. Case Stud. Therm. Eng. 2022, 33, 101957. https://doi.org/10.1016/j.csite.2022.101957.

[29] B. Sun, C. Peng, R. Zuo, D. Yang, H. Li, Investigation on the flow and convective heat transfer characteristics of nanofluids in the plate heat exchanger, Exp. Therm. Fluid Sci. 76 (2016) 75–86, https://doi.org/10.1016/j.expthermflusci.2016.03.005.

[30] M.M. Sarafraz, F. Hormozi, V. Nikkhah, Thermal performance of a counter-current double pipe heat exchanger working with COOH-CNT/water nanofluids, Exp. Therm. Fluid Sci. 78 (2016) 41–49, https://doi.org/10.1016/j.expthermflusci.2016.05.014.

[31] M. Fares, M. AL-Mayyahi, M. AL-Saad, Heat transfer analysis of a shell and tube heat exchanger operated with graphene nanofluids, Case Stud. Therm. Eng. 18 (2020) 100584, https://doi.org/10.1016/j.csite.2020.100584.

[32] A.D. Tuncer, A. Sozen, ¨ A. Khanlari, E.Y. Gürbüz, H.˙ I. Variyenli, Upgrading the performance of a new shell and helically coiled heat exchanger by using longitudinal fins, Appl. Therm. Eng. 191 (2021) 116876, https://doi.org/10.1016/j.applthermaleng.2021.116876.

[33] A.D. Tuncer, A. Sozen, ¨ A. Khanlari, E.Y. Gürbüz, H.˙ I. Variyenli, Analysis of thermal performance of an improved shell and helically coiled heat exchanger, Appl. Therm. Eng. 184 (2021) 116272, https://doi.org/10.1016/j.applthermaleng.2020.116272.

[34] R. Sheikh, S. Gholampour, H. Fallahsohi, M. Goodarzi, M. Mohammad Taheri, M. Bagheri, Improving the efficiency of an exhaust thermoelectric generator based on changes in the baffle distribution of the heat exchanger, J. Therm. Anal. Calorim. 143 (2021) 523–533, https://doi.org/10.1007/s10973-019-09253-x .
[35] Z. Tian, et al., Turbulent flows in a spiral double-pipe heat exchanger: optimal performance conditions using an enhanced genetic algorithm, Int. J. Numer. Methods Heat Fluid Flow 30 (2019) 39–53, https://doi.org/10.1108/HFF-04-2019-0287.

[36] M. Hashemian, S. Jafarmadar, H.S. Dizaji, A comprehensive numerical study on multi-criteria design analyses in a novel form (conical) of double pipe heat exchanger, Appl. Therm. Eng. 102 (2016) 1228–1237. [37] H.-Z. Han, B.-X. Li, H. Wu, W. Shao, Multi-objective shape optimization of double pipe heat exchanger with inner corrugated tube using RSM method, Int. J. Therm. Sci. 90 (2015) 173–186.

[38] M. Prithiviraj, M.J. Andrews, Three dimensional numerical simulation of shell-and-tube heat exchangers. Part I: foundation and fluid mechanics, Numer. Heat Tran. 33 (1998) 799–816.

[39] M. Prithiviraj, M.J. Andrews, Three-dimensional numerical simulation of shell-and-tube heat exchangers. Part II: heat transfer, Numer. Heat Tran. 33 (1998) 817–828.

[40] S.K. Saha, M. Baelmans, A design method for rectangular microchannel counter flow heat exchangers, Int. J. Heat Mass Tran. 74 (2014) 1–12.

[41] S.K. Saha, M. Baelmans, A design method for rectangular microchannel counter flow heat exchangers, Int. J. Heat Mass Tran. 74 (2014) 1–12.

[42] M. Zarringhalam, A. Karimipour, D. Toghraie, Experimental study of the effect of solid volume fraction and Reynolds number on heat transfer coefficient and pressure drop of CuO–water nanofluid, Exp. Therm. Fluid Sci. 76 (2016) 342–351.

[43] M.H. Esfe, S. Saedodin, O. Mahian, S. Wongwises, Heat transfer characteristics and pressure drop of COOH-functionalized DWCNTs/water nanofluid in turbulent flow at low concentrations, Int. J. Heat Mass Tran. 73 (2014) 186–194.

[44] B.-H. Chun, H.U. Kang, S.H. Kim, Effect of alumina nanoparticles in the fluid on heat transfer in double-pipe heat exchanger system, Kor. J. Chem. Eng. 25 (2008) 966–971.

[45] M.H. Esfe, S. Saedodin, O. Mahian, S. Wongwises, Heat transfer characteristics and pressure drop of COOH-functionalized DWCNTs/water nanofluid in turbulent flow at low concentrations, Int. J. Heat Mass Tran. 73 (2014) 186–194.

[46] A.A.A. Arani, J. Amani, Experimental investigation of diameter effect on heat transfer performance and pressure drop of TiO2–water nanofluid, Exp. Therm. Fluid Sci. 44 (2013) 520–533.

[47] X. Han, N. Chen, J. Yan, J. Liu, M. Liu, S. Karellas, Thermodynamic analysis and life cycle assessment of supercritical pulverized coal-fired power plant integrated with No.0 feedwater pre-heater under partial loads, J. Clean. Prod. 233 (2019) 1106–1122, https://doi.org/10.1016/j.jclepro.2019.06.159.